Vortex dynamics and angular momentum transport in accretion disks

By H. Lin, J. A. Barranco † AND P. S. Marcus ‡

1. Introduction

One of the prominent open problems in astrophysics is the mass and angular momentum transport in protoplanetary (accretion) disks. A typical disk is a few hundred AU (astronomical unit, $1\text{AU} = 1.5 \times 10^{13}\text{cm}$) in size. It is mainly composed of hydrogen and helium gas, and the thickness-to-radius ratio (aspect ratio) is usually ~ 0.1 and increases slowly with radius (a flared disk). Originating from the collapse of a rotating spherical cloud under the gravitational pull of its central star (see, *e.g.* Cassen & Moosman (1981), Terebey, Shu & Cassen (1984)), the disk has an azimuthal velocity field that can be described, provided being pressureless and steady, by the formula $V_\phi(r) = \sqrt{GM/r}$ (Keplerian velocity; here we have adopted a cylindrical coordinate system (r, ϕ, z), z is the axis of rotation, G is the constant of gravitation, and the central star of mass M can be treated as a point of gravitation at the origin for dynamics at sufficiently large radii). This velocity profile is simply given by the balance of gravitational and centrifugal force, which are the two dominant forces in the disk.

A central issue of the disk dynamics is how mass and angular momentum are radially transported. Mass accretion is supported, even though not directly confirmed, by infrared observation. However, as gas particles travel toward the star, they have to give up or transport outward their angular momentum. Because the only external force acting on the disk is the gravitation of the central star, which is no source of external torque, this transport shall only occur between parts of the disk by internal interactions. It is this mechanism that remains unknown and defines the scope of this research.

2. The averaged equation for angular momentum transport

To illustrate the problem we give a simple yet revealing analysis. Because the characteristic Reynolds number of the disk is extremely high (around 10^{14}), we can safely ignore viscosity for large scale dynamics and apply Euler's equation for the momentum as

$$\frac{D\mathbf{v}}{Dt} = -\frac{1}{\rho}\nabla p - \nabla\Phi, \tag{2.1}$$

where Φ is the gravitational potential of the central star, and the equation is described in an inertia frame. To look at the evolution of the angular momentum, we combine the azimuthal momentum equation with the continuity equation, and multiply the resulting equation by r to yield

$$\frac{\partial \rho v_\phi r}{\partial t} + \frac{1}{r}\frac{\partial \rho v_\phi v_r r^2}{\partial r} + \frac{\partial \rho v_\phi^2 r}{\partial \phi} + \frac{\partial \rho v_\phi v_z r}{\partial z} = -\frac{\partial p}{\partial \phi}. \tag{2.2}$$

† Department of Astronomy, University of California, Berkeley
‡ Department of Mechanical Engineering, University of California, Berkeley

Note that $\rho v_\phi r$ is the angular momentum, and the equation is now in conservative form. Next we define an integral operation as

$$\langle\cdot\rangle \equiv \int_{-\infty}^{+\infty}\int_0^{2\pi} \cdot\, r\mathrm{d}\phi\mathrm{d}z. \tag{2.3}$$

Under this operation equation (2.2) becomes simply

$$\frac{\partial\left\langle\rho v_\phi r\right\rangle}{\partial t} + \frac{\partial\left\langle\rho v_\phi v_r r\right\rangle}{\partial r} = 0. \tag{2.4}$$

In the integrations we have already made use of the periodicity in ϕ, and the assumption that v_z vanishes at $z = \pm\infty$. Further integrating equation (2.4) in the radial direction yields

$$\frac{\partial}{\partial t}\int_{r_1}^{r_2}\left\langle\rho v_\phi r\right\rangle \mathrm{d}r = -\left\langle\rho v_\phi v_r r\right\rangle\big|_{r=r_1}^{r=r_2}. \tag{2.5}$$

Not surprisingly, equation (2.5) reasserts angular momentum conservation in the integral form, and for an outward (or zero) angular momentum transport at a given radial location, it requires that

$$\left\langle\rho v_\phi v_r r\right\rangle \geq 0. \tag{2.6}$$

The inequality (2.6) constrains the type of flow we can have on top of the Keplerian field. To see this let us decompose the velocity field into the sum of the base Keplerian flow, and deviations from it:

$$v_\phi = V_k(r) + \tilde{v}_\phi,\;\; v_r = \tilde{v}_r, \tag{2.7}$$

where $V_k(r) \equiv \sqrt{GM/r}$, and v_z is not used in the analysis here. We also define the rate of accretion as

$$\dot{m} = -\left\langle\rho\tilde{v}_r\right\rangle, \tag{2.8}$$

which is the rate of mass flow across certain radius r, and a positive $\dot{m}$ means inward mass flow and accretion. Substituting (2.7, 2.8) into equation (2.6) yields

$$-V_k\dot{m} + \left\langle\rho\tilde{v}_\phi\tilde{v}_r\right\rangle \geq 0. \tag{2.9}$$

Equation (2.9) gives important guidance. First, for accretion ($\dot{m} > 0$), the correlation $\left\langle\rho\tilde{v}_\phi\tilde{v}_r\right\rangle$ should be positive. Second, the accretion rate suggested by observation ($\sim -10^{-9}$ to -10^{-7} solar mass per year) provides a constraint on the magnitude of the deviations through the relation (2.9), namely,

$$\left\langle\rho\tilde{v}_\phi\tilde{v}_r\right\rangle \geq V_k\dot{m}. \tag{2.10}$$

This means the flow has to transport enough angular momentum out to cancel that carried in by the accretion flow.

The next question is: what mechanism can generate a flow, with the required magnitude, sign of correlation, and most importantly, that is self-sustaining. This is the motivation of this work. The immediate candidate is a self-sustaining turbulence, possibly originating from a hydrodynamic instability. (Remember that the characteristic Reynolds number is on the order of 10^{14}.) This has become the pursuit of many works in the past decade. Nonetheless, there has not been much success in this search of turbulent flow (or any other kind of chaotic, or simply convective flow) in accretion disks, and we shall discuss this matter in the last section. While not ruling out other possibilities, our proposal in this work is that, because vortices are known to be efficient agents for transporting angular momentum, and because they are known to be ubiquitous in flows with differential rotation, we look for vortices in the accretion disks as a possible candidate of the desired flow. This we will discuss in the next section.

3. Vortex dynamics in rotating shear flow

Coherent vortices exist in both terrestrial and extraterrestrial flows. Prominent examples are the Great Red Spot on Jupiter, and the Couette-Taylor vortices which result from a instability of Couette flow between rotating cylinders. In this section we discuss their relevance to angular momentum transport, and the protoplanetary disks.

Vortices transport angular momentum in various ways. In case of the Couette-Taylor vortices, they transport angular momentum outward (toward the outer cylinder) by a positive correlation $\langle v_\phi v_r \rangle$, similar to what we have discussed in the previous section. However, the vortices themselves are stationary swirls and they do not migrate.

An alternative way is more interesting, and less discussed in the literature: vortices can move in space, and convect angular momentum as they stir the flow. Certainly in this case there exists a non-trivial correlation $\langle v_\phi v_r \rangle$ as well.

A very straightforward analysis on vortex migration is given by Schecter & Dubin (1999). In this analysis, they derived from linear theory not only the direction, but also the speed of migration of point vortices driven by a background vorticity gradient. As a result, even though the global angular momentum is conserved, the angular momentum field is convected. Before we start to discuss its relevance in the context of the disks, let us use an example in the context of geophysical flow to better illustrate the idea. We consider a channel (figure 1) in a rotating system with variable Coriolis force, known as the "$\beta-$ effect". Suppose that we are in the quasi-geostrophic regime, and the governing equation is simply given by Ertel's conservation law (see, *e.g.* Pedlosky (1987)):

$$\frac{Dq}{Dt} = \frac{\partial q}{\partial t} + u\frac{\partial q}{\partial x} + v\frac{\partial q}{\partial y} = 0, \tag{3.1}$$

where

$$q = \nabla^2 \psi - \frac{\psi}{L_R^2} + \beta y \tag{3.2}$$

is the potential vorticity, ψ is the stream function which satisfies $u = -\partial\psi/\partial y$, $v = \partial\psi/\partial x$, $\nabla^2\psi = \omega_z$, and L_R is the dimensionless Rossby deformation radius. For a flow at rest, the potential vorticity is a stationary yet non-constant field $q_b = \beta y$. It is straightforward to verify by integration by parts that

$$\frac{\partial}{\partial t}\int_A q \mathrm{d}x\mathrm{d}y = 0, \tag{3.3}$$

and

$$\frac{\partial}{\partial t}\int_A qy \mathrm{d}x\mathrm{d}y = 0, \tag{3.4}$$

where A is the section of the domain contained in the channel, and we have assumed periodicity in the x direction. Following Schecter & Dubin (1999), we define a $q-$weighted altitude as

$$\langle y \rangle = \frac{\int_A qy \mathrm{d}x\mathrm{d}y}{\int_A q \mathrm{d}x\mathrm{d}y}. \tag{3.5}$$

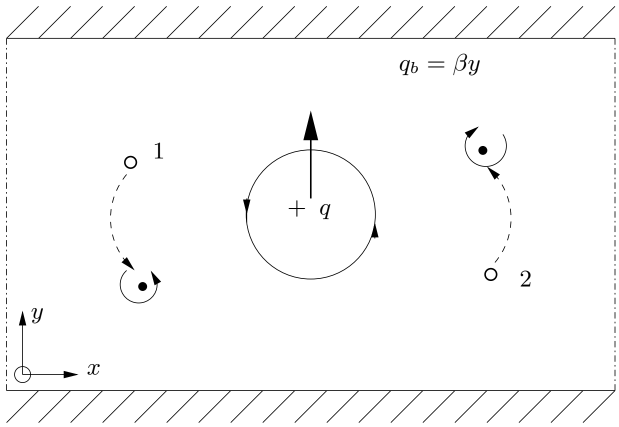

FIGURE 1. A diagram for vortex migration.

Now we may suppose that there is a constant-q patch located at the center of the flow field. Note that, a positive q-patch means a counter-clockwise circulation, a low pressure center, or a cyclone; on the other hand, a negative q-patch means a clockwise circulation, a high pressure center, or an anti-cyclone. We may decompose the $q-$weighted altitude into contributions from the background flow and the vortex patch, as

$$\langle y \rangle = \frac{\int_A q_b y \mathrm{d}x\mathrm{d}y + \int_A q_v y \mathrm{d}x\mathrm{d}y}{\int_A q \mathrm{d}x\mathrm{d}y} = \text{constant}, \tag{3.6}$$

As the vortex mixes (convects) the flow around, and because q is a material field, the contribution of the background potential vorticity q to the weighted altitude $\langle y \rangle$ is reduced. Consequently, an anti-cyclone ($q < 0$) has to move down, or an cyclone ($q > 0$) has to move up, to compensate for the change and conserve $\langle y \rangle$. (Note also that the area of the patch is preserved, from the divergence-free condition.) In these situations, the horizontal (x direction) symmetry of the vortex is clearly broken, and a non-trivial $\langle uv \rangle$ correlation has been created to exchange angular momentum. (A detailed calculation is theoretically difficult and best via numerical computation.)

The above seemingly mysterious mathematical explanation becomes clear when we take a close look at the physical processes. Take for example the case of a cyclonic vortex $q > 0$. We follow a certain particle 1 (figure 1), which has originally a zero relative vorticity (*w.r.t.* the rotating system), and which is convected down on the left side of the vortex patch by the vortex. As the βy contribution in the potential vorticity decreases along with y, the vorticity part $(\nabla^2 - 1/L_R^2)\psi$ must undergo an increase to conserve the potential vorticity. Consequently, a small cyclonic vorticity is created. Similarly a particle 2 traveling upward on the right side has its $\beta-$potential increased, and has to create a small anti-cyclonic vorticity as the compensation. The velocity field generated by these two small vorticities, which can be deduced from the Biot-Savart law, points upward on the patch. The same qualitative conclusion can be established for every point around the patch, the collective effect of the generated velocity field convects the cyclonic patch to a higher altitude, and an anti-cyclonic patch to a lower one.

This physical interpretation applies not only to the above case, but also to more general situations involving coherent vortices. We can now look at its implications to our problem at hand, which, like other more general situations, does not have the clean cut conservation laws like those of (3.3) and (3.4), and which cannot be reduced to a single variable of ψ. Nonetheless, Ertel's theorem still holds (see also Pedlosky (1987)):

$$\frac{D}{Dt}\left(\frac{\boldsymbol{\omega}}{\rho}\cdot\nabla s\right)=0, \tag{3.7}$$

where D/Dt is the material derivative, $\boldsymbol{\omega}$ is the absolute vorticity as observed in an inertia frame, and s is the specific entropy. To arrive at (3.7) only two assumption were used: i) the viscous force is ignorable, and ii) the dissipation time scale is much longer compared with the characteristic dynamics, such that entropy is material. We may further assume that the vertical vorticity ω_z and entropy gradient $\partial s/\partial z$ are the dominant ones compared with those in the azimuthal and radial directions†; then Ertel's equation becomes

$$\frac{D}{Dt}\left(\frac{\omega_z}{\rho}\frac{\partial s}{\partial z}\right)\approx 0. \tag{3.8}$$

The term $1/(\rho\partial s/\partial z)$ plays a similar role to that of βy, or the background vorticity gradient in Schecter & Dubin (1999), with its (slower) variation in the radial direction. It is the purpose of this project to study the evolution of vortices under such a thermodynamic background. (The disk has also a background vorticity gradient associated with the Keplerian flow, which influence we shall study in the future.) Certainly, the problem is much more complicated because the flow is compressible (we have a gas disk), and $\frac{1}{\rho}\frac{\partial s}{\partial z}$ is a thermodynamically evolving field rather than a static one. Our approach is outlined as the following. First, we study the general forms of long-lived (coherent) vortices in the disk. The analytical part of this problem has been given in Barranco, Marcus & Umurhan (2000), and shall not be repeated here. Second, we study the evolution of the such vortices under the influence of an entropy and density gradient in the radial direction, which are conjectured to exist in the disks. The vortices may or may not move radially, but the thermodynamic gradient can surely break their azimuthal symmetry and introduce velocity correlation. Last but not the least, we study the formation of these vortices, in part to verify the Rossby wave theory outlined in Lovelace *et al.* (1999). Currently, we are making progress on identifying various types of coherent vortices. We study the problem with numerical methods and our first results are presented in the next section.

4. Numerical scheme and results

Scalings in the protoplanetary disk is a complicated matter and was done in Barranco, Marcus & Umurhan (2000). Here we simply list the equations to solve, namely

$$\frac{\partial\bar{\rho}\mathbf{v}}{\partial t}+(\bar{\rho}\mathbf{v}\cdot\nabla)\mathbf{v}=-2\bar{\rho}\Omega\hat{k}\times(\mathbf{v}-\bar{\mathbf{v}})-\nabla\tilde{p}-\tilde{\rho}\Omega^2 z\hat{k}, \tag{4.1}$$

$$\nabla\cdot(\bar{\rho}\mathbf{v})=0, \tag{4.2}$$

$$\rho c_v\frac{DT}{Dt}=-p\nabla\cdot\mathbf{v}+\frac{T-\bar{T}}{\tau_{rad}}, \tag{4.3}$$

$$p=\rho RT \tag{4.4}$$

† Note that $\partial s/\partial z \gg \partial s\partial\phi$, $\partial s/\partial r$ is a standard assumption for optically thick disks. For the vorticity, as we will see in the next section, we will presumably set it to have a dominant component in the vertical direction. However, we do not exclude the situation that these assumptions may not be valid, and whose influence is best found through the simulations.

where the "bar-ed" quantities are the base state, which are exact solutions of the full Euler's equations, and the tilde quantities are the deviations from the base state, namely $\tilde{\rho} = \rho - \bar{\rho}$, $\tilde{p} = p - \bar{p}$. Also $\hat{k}$ is the unit vector in the z direction, R is the gas constant used in the equation of state, and Ω is the local angular velocity, *i.e.* that of the rotating frame these equations are described in.

The base state is determined judiciously by our choice of the thermodynamic background of the disk. For the current work, we will always choose a background that is stably stratified, that is to say,

$$\frac{\partial \bar{s}}{\partial z} \sim \frac{\partial}{\partial z}\left(\frac{\bar{p}}{\bar{\rho}^{\gamma}}\right) > 0. \tag{4.5}$$

The simplest way is to set the background flow to be isothermal, *i.e.* $\bar{T} = T_o = constant$. Then from the equation of state $p = \rho RT$ and hydrostatic balance in the vertical direction, one can easily obtain that

$$\bar{\rho} = \rho_o(r) \exp\left(-\frac{z^2}{2H_o^2}\right), \tag{4.6}$$

and the pressure base state is simply $\bar{\rho}RT_o$. In the above equation $\rho_o(r)$ is an arbitrary function of r whose form is determined from other physical argument (*e.g.* the well known "minimum-mass solar nebula" assumption proposed by Hayashi (1981)), and the scale height follows the standard definition $H_o \equiv c_s/\Omega$. Clearly the corresponding entropy field satisfies the requirement of stable stratification, and the density has the favorable exponentially decaying form for the assumption (to be made later) of the finite thickness of the disk. For the base state velocity, we assume that $\bar{v}$ is simply the Keplerian shear in a rotating frame, *i.e.*

$$\bar{v} = \frac{3}{2}\Omega y, \tag{4.7}$$

where y is the local radial coordinate.

The energy equation (4.3) simply manifests conservation of entropy $Ds/Dt = 0$, plus a small correction due to radiation. The radiation is naively modeled as the temperature perturbation $T - \bar{T}$ decaying on a time scale of τ_{rad}, which itself is exponentially decaying in z, *i.e.* there is more radiation toward the top and bottom layer of the disk, following an optically thick assumption. This modeling of radiation is certainly an over-simplification. However, because we are requiring that the thermodynamics does not deviate much from adiabatic process, the radiation time scale τ_{rad} is set to be very large and its effect is only detectable for very long runs†.

We solve equation (4.1-4.3) numerically with a parallel, pseudo-spectral (nonlinear terms calculated in physical space) code. The code is doubly periodic in the vertical and azimuthal direction, and Chebyshev in the radial direction. We use a time-splitting algorithm, with the leap-frog method for advection. The code is not dealiased, and equation (4.2) is satisfied through a $\tau-$method. We would like to mention that the periodicity in z is artificial, which means we are stacking identical disks on top of each other. However, as the density of the disk $\bar{\rho}$ is decaying exponentially with z, we presume that the interaction of the disks via the low density gas on the interfaces does not have a significant influence on the disk proper.

† As a matter of fact, we assume $\tau_{rad} \sim 10{,}000$ years in the middle plane at 1 AU, and $\tau_{rad} <$ year near "top" or "bottom" of the disk; however at those places the gas has very low density and the dynamical influence is presumably small.

As a side note, the immediate advantage of solving this set of equations is that the pressure operator becomes elliptical via the anelastic assumption (4.2), and is solved through a Helmholtz solver. Nonetheless when needed, we can implement a semi-implicit scheme and solve a more broadly applicable set of equations in the future.

Our first results are presented in the following.

4.1. *Coherent columnar vortices*

In this set of numerical experiments we explore semi-two-dimensional vortices. For simplicity we specify the thermodynamic background to be isothermal, and we assume that there is no radial variation in $\bar{\rho}$ and $\bar{p}$, *i.e.* $\rho_o = constant$. The radial variation will only be needed when we come to the study of vortex evolution under such a background gradient.

For each height z, we specify identically an elliptical vortex patch satisfying the Moore-Saffman formula (Saffman (1992)) for two-dimensional, steady vortices embedded in shear flow, namely

$$\frac{\tilde{\omega}_z}{\sigma} = \lambda \frac{\lambda + 1}{\lambda - 1}. \tag{4.8}$$

Here $\tilde{\omega}_z$ is the constant vorticity patch superimposed on the shear flow, $\sigma = \frac{3}{2}\Omega$ is the shear rate of the background, and $\lambda \equiv b/a$ is the ratio of the semi-axis of the elliptical patch, with b in the radial direction and a in the azimuthal direction. For a vorticity patch with a strength equal to that of the shear flow, this formula gives an aspect radio of roughly 0.5. For the vertical direction, we make the pressure and density to initially satisfy the hydrostatic balance.

The result agrees with those previously found in the two-dimensional, quasi-geostrophic cases, *e.g.* in Marcus (1993). We found that prograde vortices with a strength on the order of the background shear (or higher) maintain their coherence very well (figure 2); whereas adverse vortices or prograde vortices that are not strong enough are destroyed by the shear (figure 3). Owing to the setup of the stable stratification, the vertical velocity remained to be very small (as we put disturbances in the form of white noise to test the robustness of the vortex) in both cases. We are currently running tests to confirm that the vertical motion follows closely to that of the linear Brunt-Väisälä oscillation. These cases showed that even away from the quasi-geostrophic limit a shear flow can well support coherent vortices.

4.2. *Merger of columnar vortices*

Merging of vortices to form a larger one is speculated to be one of the possible mechanisms for the formation of coherent vortices. We demonstrate this by putting two columnar vortices in different positions of the shear flow, and let them approach each other. As we initially specify the shear flow to be positive for the upper half domain (in the radial direction) and negative in the lower half domain, the differential motion brings the vortices together, and they eventually merge to form a larger one that is of the same strength (in vorticity), but approximately double the area of the patch. The resulting vortex is again stable and coherent. This result shows that the merging of smaller vortices to form larger ones is a viable mechanism to form large, coherent vortices.

4.3. *Three-dimensional vortices*

Even though we have obtained stable forms of coherent columnar vortices, they are simply the quasi-two-dimensional analogs of two-dimensional vortices. In the environment of

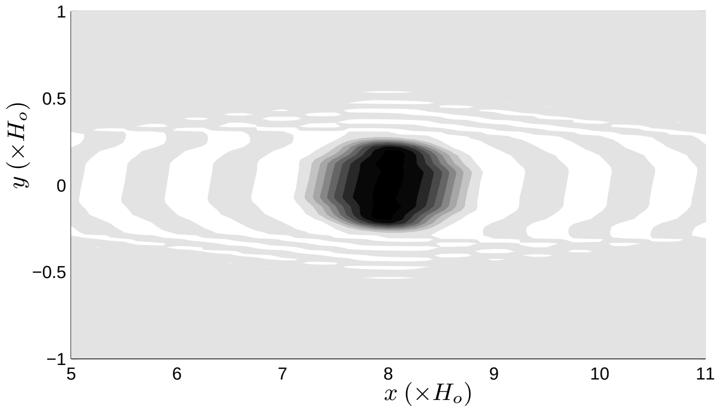

FIGURE 2. A typical stable prograde vortex. In this figure x is the local azimuthal coordinate, y is the local radial coordinate, and the contour of the vertical vorticity ω_z at the middle plane $z = 0$ is plotted. The dark elliptical patch at the center of the graph is our prograde vortex (corresponding to a vorticity "hole"). The boundary of the vortex patch oscillates with small amplitude (which is only best seen through animation), whereas the patch itself is stable. The computational resolution is $128 \times 128 \times 32$.

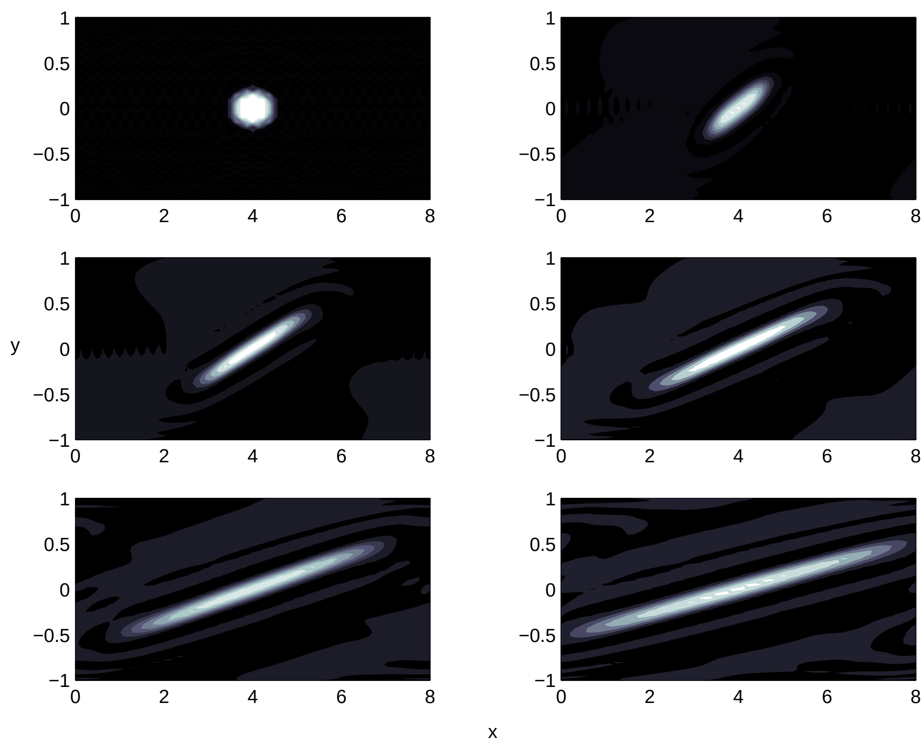

FIGURE 3. The same plot as in figure 1, but with an adverse vortex (the white patch in the first graph) instead of a prograde one. The sequence in time goes from left to right, and top to bottom; the total length of the run is about 1.6 of a turn-around time (one turn-around time equals one orbital period, or a year, in this case), and the frames are evenly divided in time. Clearly the vortex patch is stretched by the shear on the scale of turn-around time.

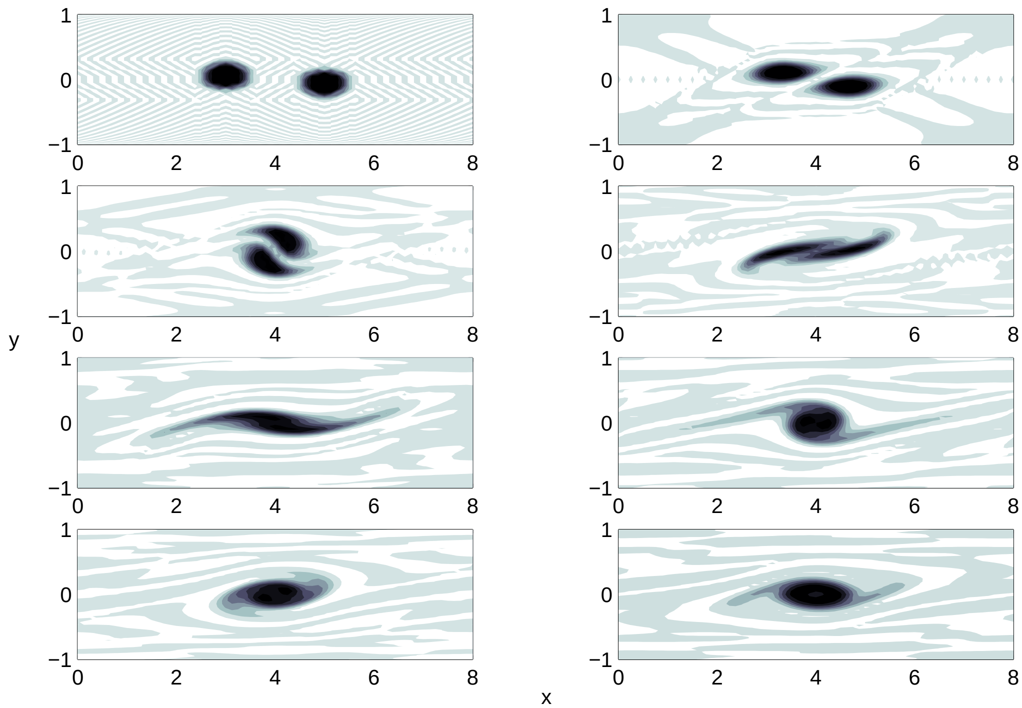

FIGURE 4. An exemplary vortex merger. As usual x and y ($\times H_o$) represent the azimuthal and radial direction, respectively. The dark patches are the prograde vorticity at the middle plane $z = 0$. Sequence in time goes from left to right, and top to bottom. The length of the run is 3 years.

the accretion disk with an order-unity Rossby number, it is of great interest to find "real" three-dimensional, coherent vortices. Three-dimensional vortices are much less understood than their two-dimensional counterparts, and much more difficult to study. Their significance lies also in their relation to planetesimal formation (see Barranco & Marcus (2000)).

Our first aim is to find pancake-like vortices, a cartoon of which can be found in figure 3 of Barranco & Marcus (2000). The character of this type of vortex is the circulation in the vertical direction within the vortex, which, we speculate, should be close to a thermal wind balance, *i.e.* the balance of the rotational effects with baroclinicity in the vertical ($r - z$) plane. We specify the initial condition to be the same as the columnar vortices in previous subsections, but reduce the strength of vorticity exponentially with height. Unfortunately, after observing similar vertical circulation pattern (as that in the cartoon) for a short duration (about a half of the turn-arounds time), the vertical cells begin to break into smaller ones, and eventually the vortex reduce in strength and decays. A possible reason can be that the background is too-strongly stratified, that a vertical circulation cannot self-sustain. Our only conclusion so far is that, the vertical setup of the background flow has a significant influence on the vortex dynamics. We will explore different combinations of thermodynamic background and vorticity initialization in the future.

5. Discussions and future work

In this report we have described the problem of angular momentum transport in the accretion disks, as well as our approach and preliminary results to this problem. Much is needed to be done in the future, following the plan we have have outlined at the end of section 3. First we need to obtain a steady form of a three-dimensional, stable vortex structure. Next, as the problem that is directly associated with the purpose of this project, we need to study the evolution of such vortices under the influence of a radial thermodynamic background, the purpose of which would be to break the azimuthal symmetry of the flow and provide a non-trivial velocity correlation to transport angular momentum.

Even though we have shown strong interest in vortex dynamics as a proposed mechanism for angular momentum transport, the possibility of the existence of turbulence (or, in general, other non-vortical flow) can never be ruled out. The Rayleigh stability criterion† can only be applied to the disk with much caution, because of complications in the disk (*e.g.* compressibility, stratification, baroclinicity, among others) that are not considered in the linear instability analysis. Furthermore, different boundary conditions easily modify the stability of a system. Nonetheless, the disk does have to satisfy some constraints, like those proposed in equations (11) and (12) in Stone & Balbus (1996); these constraints emphasize the importance of azimuthal structures (*i.e.* non-homogeneity in the azimuthal direction), without which the flow cannot be self-sustaining. In the future we will explore the possibility of turbulent flow in the disk; or, similar to the situation of the Great Red Spot on the Jupiter, that of vortices embedded in turbulent flow. Our special advantage would be that our numerical method resolves the full three-dimensional flow with vertical structures, rather than the vertical homogeneity that was assumed in Rayleigh analysis, and many other works.

Acknowledgments

The authors thank Karim Shariff, Alan Wray and Yuan-nan Young of CTR for help and very useful discussions.

REFERENCES

Barranco, J. A. & Marcus, P.S. 2000 Vortices in protoplanetary disks and the formation of planetesimals. In *Proceedings of the 2000 Summer Program.* Center for Turbulence Research, Stanford University.

Barranco, J. A., Marcus, P. S. & Umurhan, O. M. 2000 Scalings and asymptotics of coherent vortices in protoplanetary disks. *Proceedings of the 2000 Summer Program.* Center for Turbulence Research, Stanford University.

Cassen, P. & Moosman, A. 1981 On the formation of protostellar disks. *ICARUS* **48**, 353-376.

Chandrasekhar, S. 1981 *Hydrodynamic and Hydromagnetic Stability.* Dover.

Hayashi, C. 1981 Structure of the solar nebula, growth and decay of magnetic fields and effects of magnetic and turbulent viscosities on the nebula. *Prog. Theor. Phys. Suppl.* **70**, 35-53.

† See *e.g.* Chandrasekhar (1981). Because the Keplerian flow has its angular momentum increasing with radius, the criterion states that it is linearly stable.

Lovelace, R. V. E., Li, H., Colgate, S. A. & Nelson, A. F. 1999 Rossby wave instability of Keplerian accretion disks. *ApJ* **513**, 805-810.

Marcus, P. S. 1984 Simulation of Taylor-Couette flow, part 1 and 2. *J. Fluid Mech.* **146**, 45-113.

Marcus, P. S. 1993 Jupiter's Great Red Spot and other vortices. *Annu. Rev. Astron. Astrophys* **31**, 523-573.

Pedlosky, J. 1987 *Geophysical Fluid Dynamics.* Springer-Verlag.

Saffman, P. G. 1992 *Vortex Dynamics.* Cambridge University Press.

Schecter, D. A. & Dubin, D. H. E. 1999 Vortex motion driven by a background vorticity gradient. *Phys. Rev. Lett.* **83**:11, 2191-2194.

Stone, J. M. & Balbus, S. A. 1996 Angular momentum transport in accretion disks via convection. *ApJ* **464**, 264-372.

Terebey, S., Shu, F. H. & Cassen, P. 1984 The collapse of the cores of slowly rotating isothermal clouds. *ApJ* **286**, 529-551.